crystals

MDPI

Article

Mechanochemical Access to Elusive Metal Diphosphinate Coordination Polymer

Andrea Ienco [1,*], Giulia Tuci [1], Annalisa Guerri [2] and Ferdinando Costantino [3]

1 Consiglio Nazionale delle Ricerche—Istituto di Chimica dei Composti OrganoMetallici (CNR-ICCOM) Via Madonna del Piano 10, Sesto Fiorentino, I-50019 Firenze, Italy; giulia.tuci@iccom.cnr.it
2 Dipartimento di Chimica "Ugo Schiff", University of Florence, Via della Lastruccia 3, Sesto Fiorentino, I-50019 Firenze, Italy; annalisa.guerri@unifi.it
3 Dipartimento di Chimica, Biologia e Biotecnologie, University of Perugia, Via Elce di Sotto 8, I-06123 Perugia, Italy; ferdinando.costantino@unipg.it
* Correspondence: andrea.ienco@iccom.cnr.it; Tel.: +39-055-5225-282

Received: 24 April 2019; Accepted: 25 May 2019; Published: 29 May 2019

Abstract: Several binary metal diphosphinate compounds (ML) have been reported for diphosphinate bonded by a single methylene fragment. In case of longer bridges, binary products are difficult to isolate in crystalline form. Here, using a solvent assisted mechano-chemistry synthesis, we report two new ML crystalline phases, one hydrated and one anhydrous. The hydrated phase is a 2D coordination polymer with an open framework structure. Its network displays a new topology for coordination polymers and metal organic frameworks. The thermal behavior of the two phases has been studied. Finally, the importance of the bridge length is discussed in view of known metal diphosphinate compounds.

Keywords: coordination polymers; diphosphinate; copper; MOF; mechanochemistry

1. Introduction

For diphosphinates connected by a long bridge, a trio is better than a duet. We recall that phosphinates are a class of ligands widely studied in the 1960s and 1970s of the twentieth century to build inorganic polymers [1]. Nowadays, after a few decades of forgetfulness, a new use has been found for phosphinates as flame retardants, by replacing brominate polymers banned by the European Community [2]. In the last few years, phospinates have also been used as novel ligands for the synthesis of robust Metal-organic Frameworks (MOF). For instance, in 2018 Demel and co-workers used phenylene-1,4-bis(methylphosphinic acid) (PBPA) for the synthesis of porous iron(II) MOF [3]. In this study, we focus on a particular class of phosphinates, namely those with two phosphinate groups connected by an organic bridge. In the last 10 years, we have extensively studied P,P′-diphenylmethylene diphosphinic acid (H_2pcp), P,P′-diphenylethylene diphosphinic acid (H_2pc$_2$p) and P,P′-diphenyl-p-xylylene diphosphinic acid (H_2pxylp) [4,5] as shown in Scheme 1. Different diphosphinic acids were also reported [6,7].

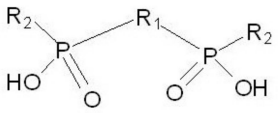

H_2pcp: R_1=-CH_2-, R_2=Phenyl

H_2pc$_2$p: R_1=-CH_2CH_2-, R_2=Phenyl

H_2pxylp: R_1= *p*-xylene, R_2=Phenyl

Scheme 1. Molecular drawing of bisphosphinate with different substituents.

In particular, the coordination ability of pcp towards alkaline earth metals [8–10], bivalent cations such tin [11] and lead [12] as well as several transition metal ions [11,13–17] are previously reported. Depending on the metal and the use of ancillary ligands, mono- [14,18] and multinuclear complexes mboxciteB19-crystals-502202,B20-crystals-502202, 1D [21–23] or 2D [21,23] coordination polymers were obtained. The isolation of two isoreticular metal organic nano tubes (MONT) built by using copper(II) metal ion, pcp and two types of bi-pyridine was one of our most interesting results [24,25], also due to the different behavior of the two materials in water. [21] On the other hand, pc_2p and pxylp ligands were found to form 2D and 3D coordination polymers easily [26–28]. One of the latter, features porous channels able to reversibly adsorb methanol [26]. Under heating, different pseudo polymorph coordination polymers have been obtained upon removal of the coordinated water molecules [26–28].

We have already discussed the different coordination ability of pcp with respect to the other diphosphinate ligands with longer bridges [20]. From the reported structures, while pcp prefers to chelate the metal atoms, the other ligands connect different metal ions with their phosphinate units [26–28] and only when a co-ligand such as 2,2′-bipy leaves free, only the *cis* positions pc_2p is found to chelate a metal center [20]. We also noticed that binary metal pcp compounds are easily obtained, while the corresponding pc_2p systems are elusive, as the common synthetic routes employed (solution or hydrothermal methods) are not satisfactory. For instance, in the case of Ni, pc_2p, bipy systems, we obtained cationic 1D chains of $[Ni(H_2O)_4(bipy)]_n^{2+}$ and dianionic diphosphinate moieties not bonding to the metal center [28].

In this work, for the first time, we were able to isolate metal pc_2p coordination polymers, using Cu(II) as metal atom using a liquid assisted mechanochemical synthesis [29]. Depending on the amount of water used, a hydrous phase of formula $[[Cu_4(pc_2p)_4(H_2O)_6]\cdot 8(H_2O)]_n$, **1**, and $Cu(pc_2p)$ anhydrous phase, **2**, were obtained. The X-ray analysis of **1** revealed a two-dimensional network with a potential porous structure, a unique characteristic in the family of the metal diphosphinate series. Topological analysis [30] was also carried out and it revealed a new topology type for **2** in the field of MOF and coordination polymers. In water **1** and **2** did not interconvert as shown by the thermal behavior of **1** and **2** studied by TGA and Temperature Dependent Powder Diffraction experiment (TDXD).

2. Materials and Methods

All reagents were analytical-grade commercial products and were used without further purification. The H_2pc_2p were prepared as previously described [31]. Elemental analyses (C, H, N) were performed with an EA 1108 CHNS-O automatic analyzer (Carlo Erba Instruments, Milan, Italy). XRD data was collected on a X'Pert PRO diffractometer (Panalytical, Almelo, the Netherlands) with Cu Kα radiation (λ = 1.5418 Å). Thermodiffractometric analysis were performed under air with an Anton Paar HTK 1200N hot chamber (Anton Paar, Graz, Austria). Thermogravimetric analyses (TGA) were performed on an EXSTAR Seiko 6200 analyzer (Seiko Instruments, Tokyo, Japan) under air (100 mL/min) at a heating rate of 10°C/min. The P/Cu ratio in 1 and 2 was measured using the X-ray (EDS) microanalysis system, Octane Elect Super Team Basic, (EDAX, AMETEK, Mahwah, NJ, USA) of a Gaia 3 (Tescan s.r.o, Brno, Czech Republic) FIB-SEM (Focused Ion Beam-Scanning Electron Microscope) Electron beam used for SEM imaging.

*2.1. Synthesis of $[[Cu_4(pc_2p)_4(H_2O)_6]\cdot 8(H_2O)]_n$, **1***

In an agate mortar, 1 mL of water was added to Cu acetate monohydrate (42 mg, 0.21 mmol). At the resulting slurry, H_2pc_2p (65 mg, 0.21 mmol) was added and grounded for 5 minutes. The product was washed with water and dried in air at room temperature. Well-formed blue crystals of **1** were obtained after several days by precipitation from a water solution (20 mL) of Cu acetate monohydrate (42 mg, 0.21 mmol) and H_2p_2pc (65 mg, 0.21 mmol). For the elemental analysis, the product dried in oven for 2 hours at 120 °C was used. The P/Cu ratio calculated using EDX is between 1.9 and 2.0 either

for the dried and the hydrated product. Yield 63 mg, 86%. $C_{28}H_{26}Cu_2O_8P_4$ (741.50 $gmol^{-1}$): calcd. C 45.36, H 3.53; found: C 45.27, H 3.59.

2.2. Synthesis of $Cupc_2p$, **2**

Cu acetate monohydrate (42 mg, 0.21 mmol) and H_2pc_2p (65 mg, 0.21 mmol) were ground with two drops of water for 5 minutes in an agate mortar. The product was washed with water and dried in air at room temperature. The P/Cu ratio calculated using EDX is between 1.9 and 2.0. Yield 55 mg, 88%. $C_{28}H_{26}Cu_2O_8P_4$ (741.50 $gmol^{-1}$): calcd. C 45.36, H 3.53; found: C 45.28, H 3.65.

2.3. X-Ray Structure Determination

A summary of the crystal data is given in Table 1. An Oxford Diffraction Excalibur 3 diffractometer (Oxford Diffraction Ltd., Abingdon, United Kingdom) equipped with Cu-Kα radiation and CCD area detector was used for data collection at 173K. The software CrysAlis CCD [32], CrysAlis RED [33] and ABSPACK [33] was employed for data collection, data reduction and absorption correction, respectively. Direct methods as coded in Sir97 [34] were used for structure solution. SHELXL program [35] was used for structure refinement on F^2 by full-matrix least squares techniques. All non-hydrogen atoms were refined anisotropically. Carbon bonded hydrogen atoms were introduced in calculated positions. The hydrogen atoms of water molecules (except the one bonded to OW5) were found in the Fourier map and refined using distance restraints. CCDC-1910569 contains the supplementary crystallographic data for this paper. These data can be obtained free of charge from the Cambridge Crystallographic Data Centre via www.ccdc.cam.ac.uk/data_request/cif.

Table 1. Crystal Data and Structure Refinement for **1**.

Empirical formula	C56 H84 Cu4 O30 P8
Formula weight	1739.15
Temperature	153(2) K
Wavelength	1.5418 Å
Crystal system	Monoclinic
Space group	P 2/c
Unit cell dimensions	a = 10.4000(10) Å
	b = 10.355(2) Å
	c = 33.277(2) Å
	β = 99.033(8)°
Volume	3539.2(8) $Å^3$
Z	2
Density (calculated)	1.632 Mg/m^3
Absorption coefficient	3.793 mm^{-1}
F(000)	1792
Crystal size	0.16 × 0.15 × 0.12 mm^3
Theta range for data collection	4.269 to 72.397°
Index ranges	−12 < = h< = 12, −12 <= k<= 12, −41 <= l < = 34
Reflections collected	55473
Independent reflections	6660 [R_{int} = 0.0430]
Completeness to θ = 26.06°	99.6%
Refinement method	Full-matrix least-squares on F^2
Data/restraints/parameters	6660/11/484
Goodness-of-fit on F^2	1.067
Final R indices [I > 2σ (I)]	R_1 = 0.0287, wR_2 = 0.0809
R indices (all data)	R_1 = 0.0337, wR_2 = 0.0847
Largest diff. peak and hole	0.451 and −0.621 e.$Å^{-3}$

3. Results and Discussion

Adding in an agata mortar 0.21 mmol of H_2pc_2p acid to a slurry of equivalent amount of copper(II) Acetate in 1 mL of water, a phase of formula $[[Cu_4(pc_2p)_4(H_2O)_6]\cdot 8(H_2O)]_n$, **1**, was obtained. The compound was recognized by the comparison of the X-ray powder diffraction

(see Figure S1 in Supplementary Materials) with the calculated pattern of the structure resolved from single crystal grown in solution.

The structure of **1** resulted in a potentially porous open framework 2D coordination polymer and its formula is $[[Cu_4(pc_2p)_4(H_2O)_6]\cdot 8(H_2O)]_n$. The asymmetric unit contains two pc_2p ligands, three independent copper atoms and nine water molecules, four of them coordinated to copper ions and five as free solvent molecules. Selected distances and angles are reported in Table 2.

Table 2. Selected bond lengths (Å) and angles (°) for **2**. Symmetry transformations used to generate equivalent atoms: #1 x + 1, y, z; #2 x, y − 1,z; #3 −x, y, −z + 1/2; #4 −x + 1, y, −z + 1/2.

Cu1-O1	1.9221(15)	Cu3-O31	1.9790(15)	O3#2-Cu1-O7#1	88.89(6)
Cu1-O5	1.9258(14)	P2-O4	1.5115(16)	O8 -Cu2-O8#3	145.44(9)
Cu1-O3#2	1.9663(15)	P3-O5	1.5141(15)	O8-Cu2-O20	107.28(5)
Cu1-O7#1	1.9313(14)	P3-O6	1.5088(15)	O8-Cu2-O21	86.82(6)
Cu1-O20	2.4651(14)	P4-O7	1.5107(15)	O8#3-Cu2-O21	93.49(6)
Cu2-O8	1.9235(14)	P4-O8	1.5087(15)	O21-Cu2-O20	89.47(5)
Cu2-O20	2.203(2)	-	-	O21-Cu2-O21#3	178.95(9)
Cu2-O21	1.9938(15)			O6-Cu3-O6#4	179.06(9)
Cu3-O6	1.9293(14)	O1-Cu1-O3#2	178.36(7)	O6-Cu3-O30	90.47(4)
Cu3-O30	2.231(3)	O1-Cu1-O5	89.84(6)	O31-Cu3-O30	92.33(5)
P1-O1	1.5115(15)	O1-Cu1-O7#1	90.52(6)	O6-Cu3-O31	87.52(6)
P1-O2	1.5121(16)	O5-Cu1-O3#2	90.95(6)	O6-Cu3-O31#4	92.44(6)
P2-O3	1.5330(15)	O5-Cu1-O7#1	172.03(6)	O31-Cu3-O31#4	175.33(9)

Two metal atoms (Cu2 and Cu3) sit on a twofold axis, while the third is in general position. Also, four oxygen atoms of water molecules are on a twofold axis. As illustrated in Figure 1a, the first pc_2p ligand is bound to two different Cu1 atoms with O1 and O3 while the other two oxygen atoms are engaged in hydrogen bonds with five different water molecules. All the oxygen atoms of the second pc_2p ligand are connected with four different copper ions, namely Cu1, Cu1', Cu2 and Cu3 (see Figure 1b). Before describing the coordination of copper atoms, it is useful to note that Cu1 metal and pc_2p ligands form a two dimensional square grid as shown in Figure 2a.

Figure 1c shows the coordination and the relation between Cu1 and Cu2 metal. Cu1 atom assumes a slightly distorted square pyramidal geometry. The basal positions are occupied by four oxygen atoms of four different pc_2p ligands, while the axial position is occupied by a water molecule with a distance Cu1-O20 of 2.4651(14)Å. The latter water is bridging between Cu1 and Cu2. The Cu2 atom is surrounded by three oxygen atoms of three water molecules and by two oxygen atoms of two different pc_2p ligands. In this case the geometry around the Cu2 atom is better described as trigonal bi-pyramidal. Finally, three oxygen atoms of three water molecules and two oxygen atoms of two different pc_2p ligand are around the Cu3 atom. A sixth water molecules is at 2.8852(6)Å as shown in Figure 1d. Interestingly, the three slightly different copper coordination in **1** is an example of how the Jahn Teller (or pseudo Jahn Teller) effect could influence the metal geometry in five coordinated complexes [36].

The pieces for building the two dimensional network are two square grids of Figure 2a on the *ab* plane and the strips formed by Cu1, Cu2 and Cu3 metal ions along *a* axis as shown in Figure 2b. The complete 2D layers are shown in Figure 2c and they have an approximate height of 16Å. The inner part presents rectangular channels of 7.7×9.2 Å^2 (excluding van der Waals radii) filled with water molecules. Excluding the solvent water molecules, the calculated void volume is 336Å^3 and it is more than the 5% of the unit cell volume. The layers are stacked together with the phenyl rings of the pc_2p ligands as shown in Figure 3c.

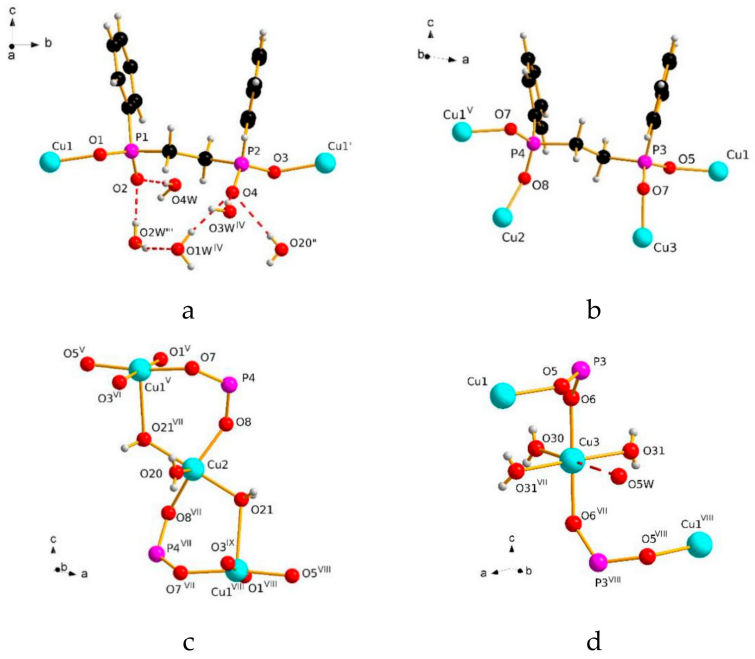

Figure 1. (**a**) Coordination mode of the first pc_2p ligand; (**b**) Coordination mode of the second pc2p ligand; (**c**) Coordination of Cu1 and Cu2; (**d**) Coordination of Cu3. Color code: Cu turquoise, P purple, O red, C grey, H white. Symmetry transformations used to generate equivalent atoms: I = x, 1 + y, z; II = 1 + x, 1 + y, z; III = 1 − x, y, ½ − z; IV = 1 + x; y, z; V = x − 1, y, z; VI = x − 1, y − 1, z; VII = −x, y, ½ − z; VIII = 1 − x, y − 1, ½ − z.

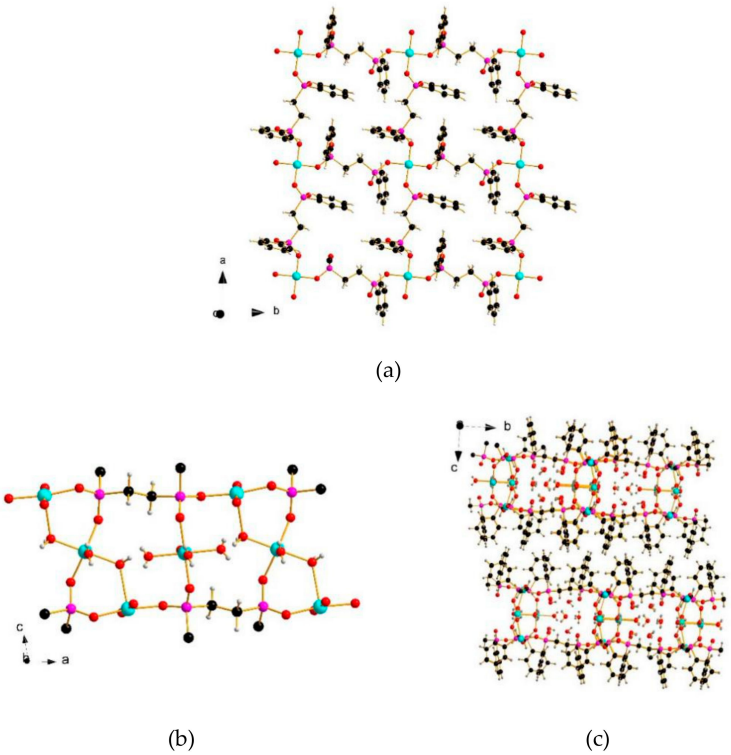

Figure 2. (**a**) Square grid formed by Cu1 and pc_2p ligands; (**b**) strips formed by by Cu1, Cu2 and Cu3 metal ions along *a* axis; (**c**) the packing of the 2D layers along the *c* axis. Color code: Cu turquoise, P purple, O red, C grey, H white.

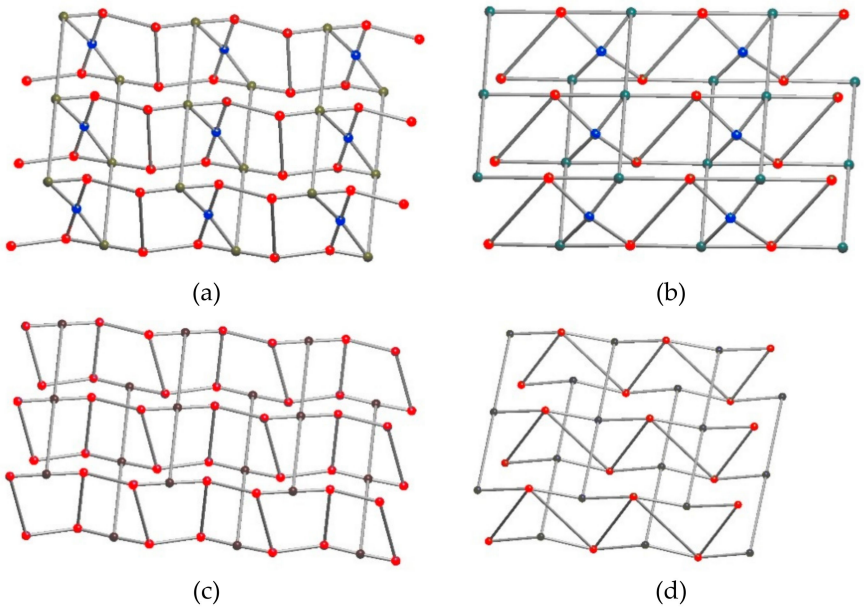

Figure 3. Schematic representation of; (**a**) 4 nodal network with two 3, one 4 and one 5 connected vertexes; (**b**) 3-nodal net with 4, 4, 5-connected vertex; (**c**) 4,4L62 and; (**d**) 3,4L156. The Cu1 node is represented in dark green, Cu3 in blue and P nodes in red.

The topological analysis was performed in order to better understand the connections in the 2D network and determine some correlation with known coordination polymers. [30,37–40] Looking at Figure 1c,d, Cu1 results in a 5-connected node, Cu2 in a 4-connected one, while Cu3 is only 2-connected and it does not contribute to the final topology. Also, the pc_2p ligand of P1 and P2 atoms is 2-connected (see Figure 1a). The other pc_2p could be considered in two different ways, in one case, in the so called standard representation, by two 3-connected nodes (P3 and P4 atoms) as shown in Figure 3a, in the other, the cluster reduction, the whole pc_2p ligand is substituted with a unique single 4-connected node (Figure 3b).

The network, represented in Figure 3a, is a 4 nodal network with two 3, one 4 and one 5 connected vertexes, while the one illustrated in Figure 3b is a 3-nodal net with a 4, 4, 5-connected vertex. The point symbols are $\{3.5.6^3.7^2.8^3\}2\{3.5.6\}2\{3^2.5^2.6^2\}\{5^2.8\}2$ and $\{3.4.5.6^6.8\}\ 2\{3.4^2.5.6^2\}\ 2\{3^2.4^2.5^2\}$ respectively. No network with this topology is present to date in the Topcryst topological database [41]. We also decided to not consider the bond between O20 and the Cu1, being longer than a normal Cu-O bond, in order to explore possible connections with other known networks. In this case, the Cu1 is a a 4-connected node, while the Cu2 is reduced to a 2-connected one. Again, the pc_2p ligand is considered formed by two 3-connected nodes in the standard representation (Figure 3c) and by a single 4 connected node in the cluster one (Figure 3d). With these choices, the network of Figure 3c is a 3-nodal net with two 3-connected and one 4 connected vertex, known as 3,4L156, while in the other case the 4,4L62 network is obtained as represented in Figure 3d. In the Topcryst database [41] two H-bonded molecular structures for 3,4L156 have been found (CCDC recodes: KEDBUS [42], EJIRIY [43]). Also, one H-bonded structure has the 4,4L62 topology (CCDC refcode ATEYII [44]). To the best of our knowledge, no covalent coordination polymer or MOF shows the same topology as **2**.

Using a different synthetic protocol, namely adding ater to a solid mixture of copper(II) Acetate and H_2pc_2p, a second phase, **2**, appeared in the powder X-ray diffraction pattern (see Figure 4d). Eventually, when just a small amount of water was used, pure **2** was synthetized. Compound **2** resulted in an anhydrous phase and it can be written as $Cu(pc_2p)$. Unfortunately, due to the poor crystallinity of the product, it was not possible to index the diffraction pattern and we were unable to obtain a single crystal of **2**.

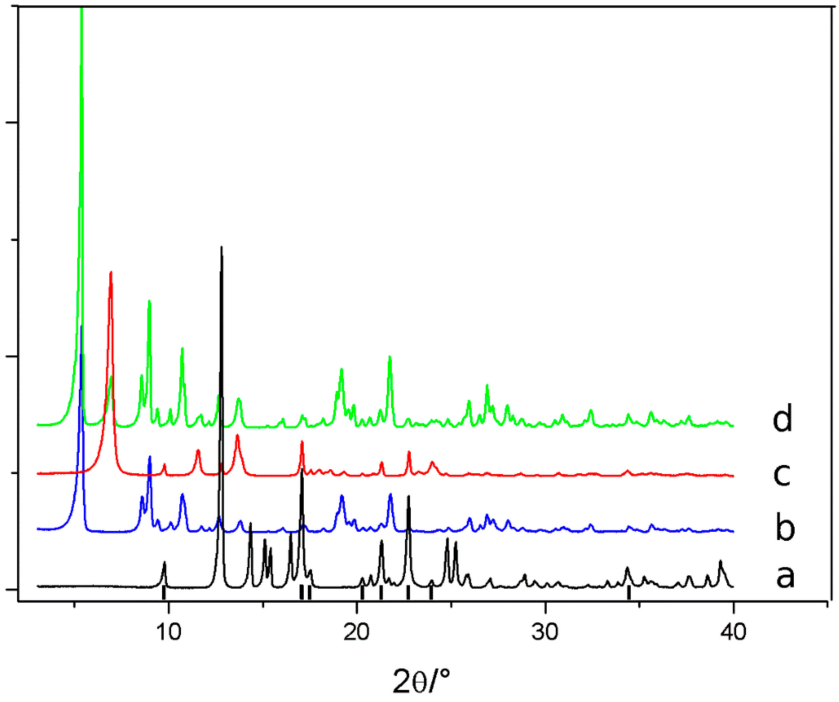

Figure 4. (**a**) Diffraction pattern of the $Cu(CH_3COO)_2$ H_2O and H_2pc_2p mixture, the main H_2pc_2p peaks in the bottom spectrum are indicated with black lines; (**b**) diffraction pattern of pure phase **1**; (**c**) diffraction pattern of pure phase **2** after the adding of few drops of water; (**d**) diffraction pattern of a mixture of **1** and **2** after the adding of 1ml of water.

The thermal behavior of the two phases was studied by thermogravimetric analysis (TGA) and temperature-dependent X-ray powder diffraction. For **1**, in the TGA under nitrogen (Figure 5a) the loss of solvent and coordinated water molecules of **1** is observed below 100 °C (14.5% calcd, 13.8% exp.). Above 200 °C, the degradation of the pc_2p ligand begins. The corresponding temperature-dependent X-ray powder diffraction patterns between 25 °C and 120 °C (Figure 5b) show a progressive meaningful shift of the first peak (0,0,2 of phase **1**) between 25 °C to 50 °C, indicating a shortening of the *c* axis. This could be interpreted as the shrinkage of the inorganic layers of **1**. In the pattern at 50 °C a new peak at around 5.9° 2θ appeared. At 70 °C, the transformation is complete as shown by the peak at 5.9° 2θ, which is attributable to an anhydrous **1**. Evidently, the latter has a different structural arrangement with respect to **2** and the loss of coordinated water results in a collapse of the inorganic layers. Phase **1** does not recover spontaneously at room temperature, but the crystallinity is restored when contacted with water. The TGA of **2** shows that the phase is stable up to 130 °C as shown in Figure 5c without any important weight loss, confirming the anhydrous nature of **2**. The temperature-dependent X-ray powder diffraction analysis between 25 °C and 120 °C shows no change in the diffraction pattern (see Figure S2 in Supplementary Materials). The total weight loss up to 800 °C is about 44% which is compatible with the thermal degradation of the organic part which occurs in two different steps (calc. 46.1% with the formula $Cupc_2p$).

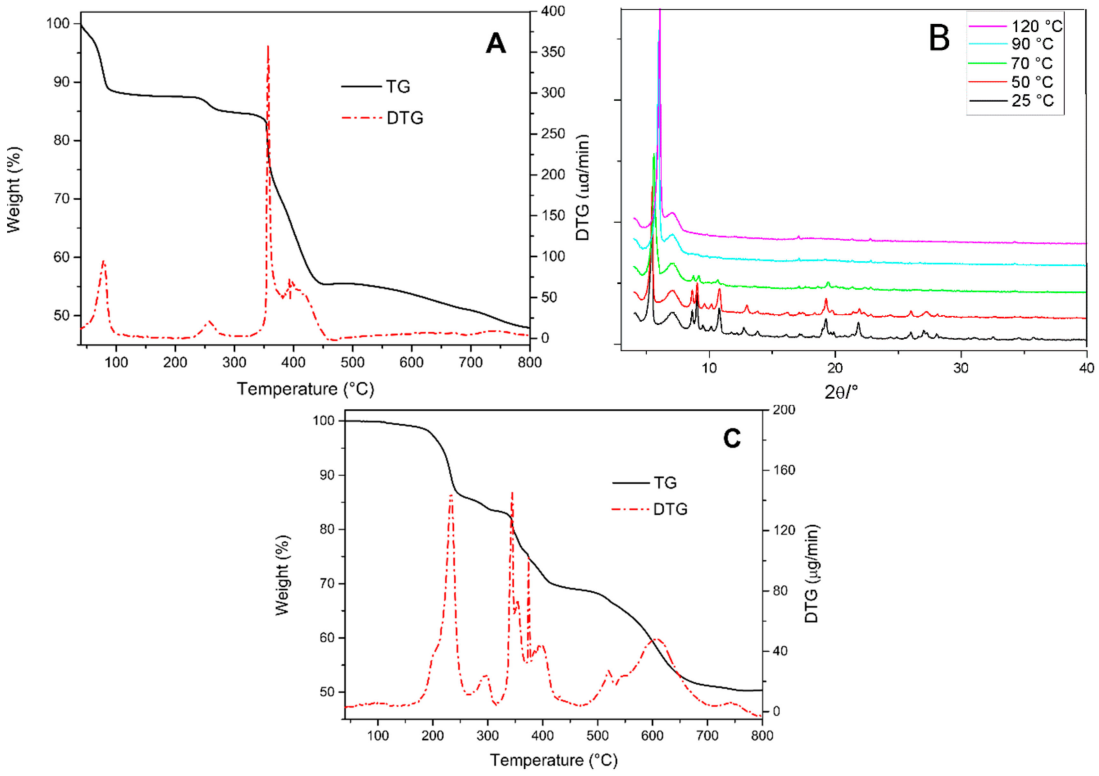

Figure 5. (**a**) TG/DTG curve of phase **1**; (**b**) temperature-dependent X-ray powder diffraction patterns for phase **1**, the peak between 6° and 8° 2θ is due to the diffraction of Kapton® polymer used as window in the Anton-Paar Hot Chamber; (**c**) TG/DTG curve of phase **2**.

Finally using CSD database surveys [45], we wanted to confirm the higher tendency of pcp for metal chelation compared to the pc_2p ligand. Only in three cases out of 28, pcp does not chelate to at least one metal center. The result is reversed for pc_2p (2 out of 7). The two examples are with a 2,2′-bipy co-ligand where they leave free only the cis positions around the metal center for the metal coordination of the pc_2p [20]. Another geometrical parameter is also investigated, namely the CPPC dihedral angle between the two phenyl rings bonded to the phosphorus atoms. For the 37 examples found, the average value is 28° for pcp with only three outliers with angles greater than 110°. Again, for pc_2p, the result is reversed. The mean value for the angle is 148° (15 examples) with only an outlier with an angle of 18°. So, the different behavior in metal coordination as well as in the ability of forming network and coordination polymers can be related to the different structural capability given by the nature of the bridge between the two phosphinate groups.

4. Conclusions

Using a solvent assisted mechano chemistry synthesis, two new binary phases between copper and pc_2p were been isolated. One of them was anhydrous material, while the other was found to be a peculiar 2D coordination polymer. Two square slabs were connected together by a copper metal center, forming potential voids filled by solvent water molecules. From the topological analysis, the 2D network revealed an unknown topology for coordination polymers, also when different kinds of network simplifications was considered. The thermal behavior of the two phases was studied. The collapse of the 2D network was confirmed, but the anhydrous phase obtained was different from the one directly obtained in the synthesis. A database survey on the known pcp and pc_2p structures demonstrated how the nature of the bridging chain between the phosphinate group is a key factor for the resulting structure.

Supplementary Materials: The following are available online at http://www.mdpi.com/2073-4352/9/6/283/s1, Figure S1: Comparison of the calculated and experimental X-ray pattern for **1**; Figure S2: Temperature-dependent X-ray powder diffraction patterns for phase **2**.

Author Contributions: Conceptualization, A.I. and F.C.; investigation, A.I., G.T., A.G., F.C.; writing—original draft preparation, A.I.; writing—review and editing, A.I., G.T., A.G., F.C.

Funding: This research received no external funding.

Acknowledgments: A.I. acknowledges Carlo Bartoli for his technical assistance. The authors thank the Italian National Research Council (CNR) microscopy facility "Ce.M.E.–Centro Microscopie Elettroniche Laura Bonzi" for the experiments on Gaia 3, instrument acquired thanks to "Ente Cassa di Risparmio di Firenze" Grant Number n. 2013.0878 and Regione Toscana POR FESR 2014-2020 for the project FELIX (Fotonica ed Elettronica Integrate per l'Industria), Grant Number 6455.

Conflicts of Interest: The authors declare no conflict of interest.

References

1. Vioux, A.; Le Bideau, J.; Mutin, P.H.; Leclercq, D. Hybrid Organic-Inorganic Materials Based on Organophosphorus Derivatives. In *New Aspects in Phosphorus Chemistry IV. Topics in Current Chemistry*; Majoral, J.P., Ed.; Springer: Berlin/Heidelberg, Germany, 2004; Volume 232, pp. 145–174.
2. Wendels, S.; Chavez, T.; Bonnet, M.; Salmeia, K.; Gaan, S. Recent developments in organophosphorus flame retardants containing P-C bond and their applications. *Materials* **2017**, *10*, 784. [CrossRef]
3. Hynek, J.; Brázda, P.; Rohlíček, J.; Londesborough, M.; Demel, J. Phosphinic Acid Based Linkers: Building Blocks in Metal–Organic Framework Chemistry. *Angew. Chem. Int. Ed.* **2018**, *57*, 5016–5019. [CrossRef]
4. Costantino, F.; Ienco, A.; Taddei, M. Hybrid Multifunctional Materials Based on Phosphonates, Phosphinates and Auxiliary Ligands. In *Tailored Organic-Inorganic Materials*; Brunet, E., Colon, J.L., Clearfield, A., Eds.; John Wiley & Sons: Hoboken, NJ, USA, 2015; pp. 193–244.
5. Costantino, F.; Ienco, A.; Taddei, M. The Influence of Non-covalent Interactions in the Structure and Dimensionality of Hybrid Compounds and Coordination Polymers in Non-Covalent Interactions. In *Synthesis and Design of New Compounds*; Maharramov, A.M., Mahmudov, K.T., Kopylovich, M.N., Pombeiro, A.J.L., Eds.; John Wiley & Sons: Hoboken, NJ, USA, 2016; pp. 163–184.
6. David, T.; Procházková, S.; Kotek, J.; Kubíček, V.; Hermann, P.; Lukeš, I. Aminoalkyl-1,1-bis(phosphinic acids): Stability, acid-base, and coordination properties. *Eur. J. Inorg. Chem.* **2014**, *2014*, 4357–4368. [CrossRef]
7. David, T.; Procházková, S.; Havlíčková, J.; Kotek, J.; Kubíček, V.; Hermann, P.; Lukeš, I. Methylene-bis[(aminomethyl)phosphinic acids]: Synthesis, acid-base and coordination properties. *Dalton Trans.* **2013**, *42*, 2414–2422. [CrossRef] [PubMed]
8. Cecconi, F.; Dominguez, S.; Masciocchi, N.; Midollini, S.; Sironi, A.; Vacca, A. Complexation of beryllium(II)ion by phosphinate ligands in aqueous solution. Synthesis and XRPD structure determination of $Be[(PhPO_2)_2CH_2](H_2O)_2$. *Inorg. Chem.* **2003**, *42*, 2350–2356. [CrossRef]
9. Midollini, S.; Lorenzo-Luis, P.; Orlandini, A. Inorganic-organic hybrid materials of p,p′-diphenylmethylenediphosphinic acid (H_2pcp) with magnesium and calcium ions: Synthesis and characterization of $[Mg(Hpcp)_2]$, $[Mg(Hpcp)_2(H_2O)_4]$, $[Mg(pcp)(H_2O)_3](H_2O)$, $[Ca(Hpcp)_2]$ and $[Ca(pcp)(H_2O)]$ complexes. *Inorg. Chim. Acta* **2006**, *359*, 3275–3282. [CrossRef]
10. Costantino, F.; Gentili, P.; Guerri, A.; Ienco, A.; Midollini, S.; Oberhauser, W. Structural similarities in 1D coordination polymers of alkaline earth diphosphinates. *Inorg. Chim. Acta* **2012**, *391*, 150–157.
11. Beckmann, J.; Costantino, F.; Dakternieks, D.; Duthie, A.; Ienco, A.; Midollini, S.; Mitchell, C.; Orlandini, A.; Sorace, L. Inorganic-organic hybrids of the p,p′-diphenylmethylenediphosphinate, pcp^{2-}. Synthesis, characterization, and XRPD structures of [Sn(pcp)] and [Cu(pcp)]. *Inorg. Chem.* **2005**, *44*, 9416–9423.
12. Cecconi, F.; Ghilardi, C.; Midollini, S.; Orlandini, A. A new lead(II) inorganic-organic hybrid of the P,P′-diphenylmethylene-diphosphinate ligand: Synthesis and X-ray characterization of the $[Pb(CH_2(P(Ph)O_2)_2)]$ complex. *Inorg. Chem. Commun.* **2003**, *6*, 546–548. [CrossRef]
13. Lyssenko, K.A.; Vologzhanina, A.V.; Torubaev, Y.V.; Nelyubina, Y.V. A comparative study of a mixed-ligand Copper(II) complex by the theory of atoms in molecules and the Voronoi tessellation. *Mendeleev Commun.* **2014**, *24*, 216–218. [CrossRef]

14. Ciattini, S.; Costantino, F.; Lorenzo-Luis, P.; Midollini, S.; Orlandini, A.; Vacca, A. Inorganic-organic hybrids formed by p,p′- diphenylmethylenediphosphinate, pcp^{2-}, with the Cu^{2+} ion. x-ray crystal structures of $[Cu(pcp)H_2O_2]\cdot H_2O$ and $[Cu(pcp)bipy(H_2O)]$. *Inorg. Chem.* **2005**, *44*, 4008–4016. [CrossRef]
15. Cecconi, F.; Dakternieks, D.; Duthie, A.; Ghilardi, C.; Gili, P.; Lorenzo-Luis, P.; Midollini, S.; Orlandini, A. Inorganic-organic hybrids of the p,p′-diphenylmethylenediphosphinate ligand with bivalent metals: A new 2D-layered phenylphosphinate zinc(II) complex. *J. Solid State Chem.* **2004**, *177*, 786–792. [CrossRef]
16. Berti, E.; Cecconi, F.; Ghilardi, C.; Midollini, S.; Orlandini, A.; Pitzalis, E. Isostructural organic-inorganic hybrids of P,P′-diphenyl-methylenediphosphinate $(CH_2(P(Ph)O_2)_2)^{2-}$ with divalent transition metals. *Inorg. Chem. Commun.* **2002**, *5*, 1041–1043.
17. Costantino, F.; Midollini, S.; Orlandini, A.; Sorace, L. Hydrothermal synthesis and structural characterization of a new 2D-layered vanadium diphosphinate: $[VO(O_2(C_6H_5)PCH_2P(C_6H_5)O_2)]$. *Inorg. Chem. Commun.* **2006**, *9*, 591–594. [CrossRef]
18. Midollini, S.; Orlandini, A. Hydrogen bonding in triamine copper(II) P,P′- Diphenyl methylene diphosphinate (pcp^{2-}) hybrids. Syntheses and crystal structures of $[Cu(pcp)(2,2'$-dipyridylamine$)(H_2O)]\cdot 2H_2O$ and $[Cu(pcp)(2,2':6',2''$terpyridine$)]\cdot 4\ H_2O$. *J. Coord. Chem.* **2006**, *59*, 1433–1442. [CrossRef]
19. Ienco, A.; Midollini, S.; Orlandini, A.; Costantino, F. Synthesis and structural characterization of a tetranuclear zinc(II) complex with P,P′-diphenylmethylenediphosphinate (pcp) and 2,2′-bipyridine (2,2′-bipy) ligands. *Z. Naturforsch. B Chem. Sci.* **2007**, *62*, 1476–1480. [CrossRef]
20. Costantino, F.; Ienco, A.; Midollini, S.; Orlandini, A.; Sorace, L.; Vacca, A. Copper(II) complexes with bridging diphosphinates—The effect of the elongation of the aliphatic chain on the structural arrangements around the metal centres. *Eur. J. Inorg. Chem.* **2008**, *2008*, 3046–3055. [CrossRef]
21. Taddei, M.; Ienco, A.; Costantino, F.; Guerri, A. Supramolecular interactions impacting on the water stability of tubular metal-organic frameworks. *RSC Adv.* **2013**, *3*, 26177–26183. [CrossRef]
22. Ienco, A.; Caporali, M.; Costantino, F.; Guerri, A.; Manca, G.; Moneti, S.; Peruzzini, M. The quest for hydrogen bond-based metal organic nanotubes (MONT). *J. Coord. Chem.* **2014**, *67*, 3863–3872. [CrossRef]
23. Costantino, F.; Midollini, S.; Orlandini, A. Cobalt(II) and nickel(II) coordination polymers constructed from P,P′-diphenylmethylenediphosphinic acid (H_2pcp) and 4,4′-bipyridine (bipy): Structural isomerism in $[Co(pcp)(bipy)_{0.5}(H_2O)_2]$. *Inorg. Chim. Acta* **2008**, *361*, 327–334. [CrossRef]
24. Bataille, T.; Costantino, F.; Lorenzo-Luis, P.; Midollini, S.; Orlandini, A. A new copper(II) tubelike metal-organic framework constructed from P,P′-diphenylmethylenediphosphinic acid and 4,4′-bipyridine: Synthesis, structure, and thermal behavior. *Inorg. Chim. Acta* **2008**, *361*, 9–15. [CrossRef]
25. Bataille, T.; Bracco, S.; Comotti, A.; Costantino, F.; Guerri, A.; Ienco, A.; Marmottini, F. Solvent dependent synthesis of micro-and nano-crystalline phosphinate based 1D tubular MOF: Structure and CO_2 adsorption selectivity. *CrystEngComm* **2012**, *14*, 7170–7173. [CrossRef]
26. Bataille, T.; Costantino, F.; Ienco, A.; Guerri, A.; Marmottini, F.; Midollini, S. A snapshot of a coordination polymer self-assembly process: The crystallization of a metastable 3D network followed by the spontaneous transformation in water to a 2D pseudopolymorphic phase. *Chem. Commun.* **2008**, *2008*, 6381–6383. [CrossRef] [PubMed]
27. Costantino, F.; Ienco, A.; Midollini, S. Different structural networks determined by variation of the ligand skeleton in copper(II) diphosphinate coordination polymers. *Cryst. Growth Des.* **2010**, *10*, 7–10. [CrossRef]
28. Guerri, A.; Taddei, M.; Bataille, T.; Moneti, S.; Boulon, M.; Sangregorio, C.; Costantino, F.; Ienco, A. Same Not the Same: Thermally Driven Transformation of Nickel Phosphinate-Bipyridine One-Dimensional Chains into Three-Dimensional Coordination Polymers. *Cryst. Growth Des.* **2018**, *18*, 2234–2242. [CrossRef]
29. Bowmaker, G.A. Solvent-assisted mechanochemistry. *Chem. Commun.* **2013**, *49*, 334–348.
30. Alexandrov, E.V.; Shevchenko, A.; Blatov, V.A. Topological databases: why do we need them for design of coordination polymers? *Cryst. Growth Des.* **2019**. [CrossRef]
31. Garst, M.E. Alkylation of Phenyl Phosphinic Acid. *Synth. Commun.* **1979**, *9*, 261–266. [CrossRef]
32. *CrysAlisCCD*; Version1.171.33.41 (release06-05-2009 CrysAlis171.NET); Oxford Diffraction Ltd.: Abingdon, UK, 2009.
33. *CrysAlisRED*; Version1.171.33.41 (release06-05-2009 CrysAlis171.NET); Oxford Diffraction Ltd.: Abingdon, UK, 2009.

34. Altomare, A.; Burla, M.C.; Camalli, M.; Cascarano, G.L.; Giacovazzo, C.; Guagliardi, A.; Moliterni, A.G.G.; Polidori, G.; Spagna, R. SIR97: A new tool for crystal structure determination and refinement. *J. Appl. Crystallogr.* **1999**, *32*, 115–119. [CrossRef]
35. Sheldrick, G.M. A short history of SHELX. *Acta Crystallogr. Sect. A Found. Crystallogr.* **2008**, *64*, 112–122. [CrossRef]
36. Bacci, M. Jahn-Teller effect in five-coordinated copper(II) complexes. *Chem. Phys. Lett.* **1986**, *104*, 191–199. [CrossRef]
37. Bonneau, C.; O'Keeffe, M.; Proserpio, D.; Blatov, V.; Batten, S.; Bourne, S.; Lah, M.; Eon, J.; Hyde, S.; Wiggin, S.; et al. Deconstruction of Crystalline Networks into Underlying Nets: Relevance for Terminology Guidelines and Crystallographic Databases. *Cryst. Growth Des.* **2018**, *18*, 3411–3418. [CrossRef]
38. Blatov, V.A.; Shevchenko, A.P.; Proserpio, D.M. Applied Topological Analysis of Crystal Structures with the Program Package ToposPro. *Cryst. Growth Des.* **2014**, *14*, 3576–3586. [CrossRef]
39. Alexandrov, E.V.; Blatov, V.A.; Kochetkov, A.V.; Proserpio, D.M. Underlying nets in three-periodic coordination polymers: topology, taxonomy and prediction from a computer-aided analysis of the Cambridge Structural Database. *CrystEngComm* **2011**, *13*, 3947–3958. [CrossRef]
40. Mitina, T.G.; Blatov V., A. Topology of 2-Periodic Coordination Networks: Toward Expert Systems in Crystal Design. *Cryst. Growth Des.* **2013**, *13*, 1655–1664. [CrossRef]
41. TOPCryst Topological Database. Available online: https://topcryst.com/ (accessed on 14 April 2019).
42. Sachdeva, N.; Dolzhenko, A.; Keung Chui, W. Regioselective synthesis of pyrimido[1,2-a][1,3,5]triazin-6-ones via reaction of 1-(6-oxo-1,6-dihydropyrimidin-2-yl)guanidines with triethylorthoacetate: Observation of an unexpected rearrangement. *Org. Biomol. Chem.* **2012**, *10*, 4586–4596. [CrossRef]
43. Wu, Y.-J.; He, H.; Sun, L.-Q.; Wu, D.; Gao, Q.; Li, H.-Y. Synthesis of fluorinated 1-(3-Morpholin-4-yl-phenyl)-Ethylamines. *Bioorg. Med. Chem. Lett.* **2003**, *13*, 1725–1728. [CrossRef]
44. Li, C.; An, C.; Li, X.; Gao, S.; Cui, C.; Sun, H.; Wang, B. Triazole and Dihydroimidazole Alkaloids from the Marine Sediment-Derived Fungus Penicillium paneum SD-44. *J. Nat. Prod.* **2011**, *74*, 1331–1334. [CrossRef]
45. Groom, C.R.; Bruno, I.J.; Lightfoot, M.P.; Ward, S.C. The Cambridge Structural Database. *Acta Cryst.* **2016**, *B72*, 171–179. [CrossRef]

© 2019 by the authors. Licensee MDPI, Basel, Switzerland. This article is an open access article distributed under the terms and conditions of the Creative Commons Attribution (CC BY) license (http://creativecommons.org/licenses/by/4.0/).